

Considerations in Phase-Doppler Measurements of Spray/Wall Interaction

Davood Kalantari¹, Cameron Tropea²

1: Institute of Fluid Mechanics and Aerodynamics, TU-Darmstadt, d.kalantari@sla.tu-darmstadt.de

2: Chair of Fluid Mechanics and Aerodynamics, TU-Darmstadt, ctropea@sla.tu-darmstadt.de
Petersenstr. 30, 64287 Darmstadt, Germany

Abstract In this work, an experimental study of spray impact onto a horizontal flat and rigid surface is presented to specify the suitable measurement volume height above the surface in which the Phase-Doppler measurements are valid. Furthermore the influence of the input laser power on the characteristics of the impinging and secondary spray is studied in detail. The phase Doppler technique has then been used to characterise both the impacting and the secondary spray in terms of number flux, size distribution and velocities of the droplets above the target. A high-speed CCD camera has been used to characterize the splashing or rebounding droplets and to measure the average film thickness formed due to spray impact. In this paper some new considerations in Phase-Doppler measurements of spray-wall interaction are presented.

Keywords: spray; spray impact; secondary spray; Phase-Doppler; interaction.

1. Introduction

The interest in a reliable modelling of spray/wall interaction is widespread, focussing on the prediction of the deposited mass fraction and the characteristics of the secondary spray. Important applications include fuel injection and spray cooling. For formulation and verification of suitable models, experiments under well-controlled conditions are essential.

For precisely capturing the secondary spray, physical and morphological characteristics of the spray impact phenomena, including different sources for generation of the secondary spray, should be clearly understood and considered when employing a Phase-Doppler measurement of a spray/wall interaction.

The spray impact onto a rigid wall consists of many individual droplet impacting onto the rigid wall or liquid film and different interactions. In spray impact phenomena, secondary droplets are generated from: splashing droplets, ejected wall films, and rebounded droplets from the wall (Fig. 1). Interactions in a spray take place between: two droplets (two in-going drops, in-going and ejecting drops or two secondary droplets); an uprising jet and a drop; and a splashing droplet and other droplet (ingoing or ejecting droplet).

Impacting droplets are deposited on the wall at very low impact energy (i.e., $We_{nb} < 2$), generating the wall film. Partial deposition occurs also at higher impact Weber numbers, i.e. $30 < We_{nb} < 80$, when the spreading droplet loses its kinetic energy due to dissipation at the boundary layer of the spreading droplet.

At relative low energetic impact conditions, impacting droplets can rebound from the wall. A droplet rebounds from the wall if the surface energy of the droplet at the end of partial spreading is larger than the kinetic and surface energy of the impacting droplet minus the viscous energy dissipation during the spreading. Threshold criteria is given by Bai and Gosman (1995) for "Rebound-deposition" as $We_{nb} = 5$ ($We_{nb} = \rho u^2 d / \sigma$, where u is the normal velocity component before impact) based on the result of an isolated single drop impact, or $We_{nb} = 20$ for spray impact conditions based on the observation of Lee and Hanratty (1988) and Ching et al. (1984). Also the observations of Wang and Watkins (1993) show that rebound occurs only for $We_{nb} < 30$.

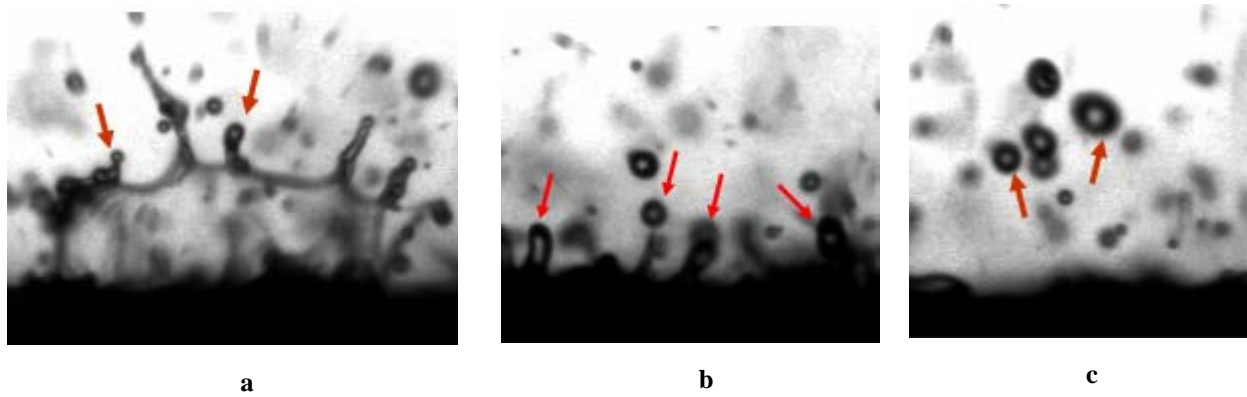


Fig.1: Different origins of secondary droplets and formation of liquid film on the wall: secondary droplet ejected from: a) splashing droplet, b) ejected wall film, and c) rebounded droplet.

Drop rebound is also observed for oblique impacts, whereby the threshold criterion is generally considered still valid if only the normal component of velocity is used in computed the impact Weber number, Sikalo et al. (2005).

Splashing occurs at higher values of the normal impact Weber number, $We_{nb} > 80$ and it appears that the tangential velocity component does not play any important role in the onset of splashing. Physically, splashing or break-up of a droplet occurs in the final stage of spreading. This occurs when the total energy of a droplet at the final stage of spreading is larger than its surface energy. Structure of a splashing droplet consists of a thin crown-like liquid sheet (crown body). This crown-like sheet is bounded with a free end rim due to the capillary effect, which generates finger-like jets disintegrating into the very small secondary droplets. Observation of Coghe et al. (1999) shows that each splashing drop generates at least 10 tiny droplets.

The limit of impact Weber number for onset of splashing also depends on the some additional parameters such as surface roughness and average depth of accumulated liquid film on the wall, e.g. splashing takes place faster for rough surfaces as postulated by Mundo et al. (1998). Also it is shown by Cossali et al. (1997) that in the case of a single drop impact onto a stationary liquid film, the number of secondary droplets decreases as the depth of liquid layer is increased. Four different liquid film regimes are classified based on a threshold Weber number (We_{th}) required for the onset of splashing by Kalantari and Tropea (2006). The value of Weber number required for the onset of splashing is constant for the case of $\bar{h}^* \leq 0.1$ (wetted wall) as proposed by Schmehl et al. (1998). The threshold Weber number then increases monotonically with an increase of the dimensionless film thickness up to $\bar{h}^* = 1$ (thin liquid film) and then decreases until $\bar{h}^* = 2$ (shallow liquid film) and finally takes an asymptotic value corresponding to a deep liquid layer (deep pool condition).

The integration of experimental data into numerical predictions in the form of empirical models or verification of the predictions requires taking into account the gradients in Phase Doppler measurements of the spray/wall interaction. The present work provides such experimental results indicating the influence of the measurement volume height above the rigid wall, the influence of the input laser power on the characteristics of the impinging and secondary spray and considerations for spatial location of the detected impinging and secondary spray.

2. Experimental set-up

The experimental set-up used in this work is pictured in Fig.2. The spray was created using two different full cone nozzles from Spraying System Co., operated at pressures between 2 and 7 bars.

Both flow rate and pressure during the experiments were variable and measured. A stainless steel target with diameter of 5mm has been used in this study, using the end face of the cylinder.

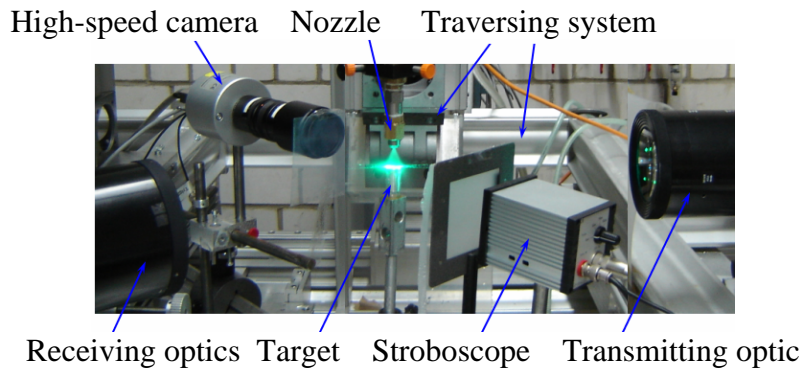


Fig.2: Photograph of experimental set-up used in this study.

The nozzles were placed at different positions above the target surface from 20 to 50 mm, e.g. ($x_{nozzle} = -20$ mm). To characterise the spray, a dual-mode phase Doppler instrument from Dantec Dynamics was used, comprising a transmitting optics with a 310mm focal length, a receiving optics with a 310mm focal length, and an “A” type mask at a 36° scattering angle. By using a dual-mode configuration both normal and tangential velocity components of each individual droplet and its diameter were measured by placing the measurement volume 0.25mm to 2.5mm above the target surface (e.g., $x = -1$ mm). The in-going and out-going droplets are distinguished using the sign of the velocity component normal to the target, i.e. positive u denotes an impacting droplet and a negative u denotes a secondary droplet.

The overall size distributions were corrected for the size dependent detection volume cross-section using the standard system software. Experimentally the accumulated wall film has been characterised using a high-speed CCD camera. The average wall film thickness (\bar{h}) is obtained by averaging over several instantaneous images after first removing the reference wall image.

3. Results and discussion

The most obvious difficulty is to specify the measurement volume height above the surface at which the phase Doppler data is valid. In Fig.3a and b, the dependence of velocity before the impact and velocity after the impact are illustrated as a function of measurement height above the wall. This data has been taken in a reasonably sparse spray impacting onto a flat target with a relatively thin film. It illustrates that both the in-coming spray and the secondary spray can exhibit strong gradients in the wall normal direction. Although numerical simulations of the spray and the gas flow can capture such gradients, the synchronisation between experiment and simulations, either for model calibration or for verification of predictions, must take these gradients into account.

Results presented in Fig.3a indicate that the mean velocity before the impact increase significantly with the measurement volume height above the wall. Also these results indicate that the mean impact velocity decrease with the input laser power. The influence of the laser power on the mean drop impact velocity is stronger (larger) at lower laser powers, as illustrated in Fig. 3a.

Other results presented in Fig.3b indicate that the average velocity after the impact increases with the measurement volume height up to 2 mm, then doesn't change significantly after it. Influence of the laser power on the average velocity after the impact is not significant, as presented in Fig. 3b.

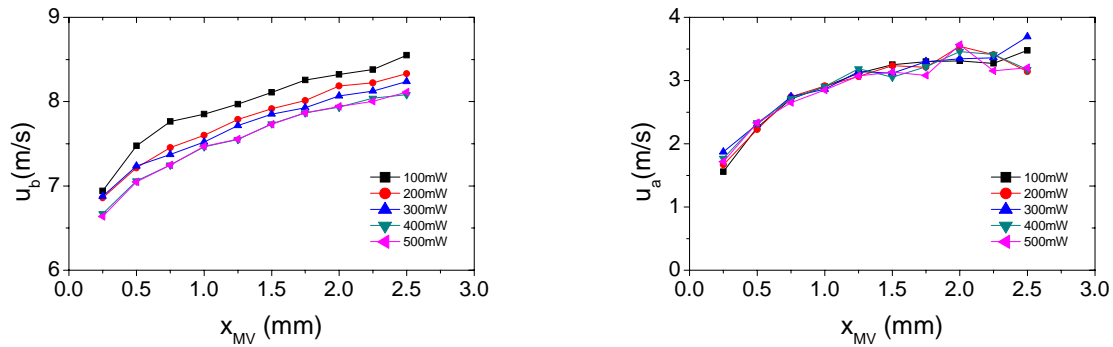


Fig. 3: Mean velocity a) before the impact and b) after the impact, as a function of measurement volume height above the rigid wall. The different lines represent different laser power.

The influence of the measurement volume height above the rigid wall on the measured average drop size before and after impact are presented in Fig.4a and b. Results indicate that the average drop size before the impact decrease with measurement volume height above the target up to 1 mm, but doesn't change significantly after $x=1$ mm. Large difference in measuring the average drop size before the impact at laser power=100 mW and other values of the laser power can be observed in Fig. 4a. This result can be important when measuring dense or ultra-dense sprays, in which the laser power at the both sides of the spray is not uniform. In other words, the laser intensity at the center of measurement volume can decrease significantly due to increasing the absorption and scattering the laser light by moving particles at the opposite side of the laser beams entering the liquid spray, i.e., opposite side of the transmitting optic. Therefore a calibration for Phase-Doppler measurements is required at both sides of the dense sprays to obtain a reliable result. The influence of the laser power on the average drop size before the impact is significant in which d_{10b} decreases with increasing the laser power (Fig.5).

The influence of the measurement volume height on average drop size after the impact is more complicated. The value of d_{10a} decreases at first with a measurement volume height up to 1.5 mm, then increases with the measurement volume height above the target. Based on the results presented in Fig. 4b, the larger average secondary drop size very close to the wall can be due to the absence of the very small droplets generated from splashing droplets, since secondary droplets generated by splash cannot be captured very close to the wall. Increasing the average secondary drop size after a certain height above the wall, e.g. after $x_{MV}=1.5$ mm in this figure, can be due to interaction of the secondary droplets with other droplets and deposition of the generated secondary droplets due to larger trajectory angles and smaller velocity components normal to the wall. The influence of the laser power on the average after impact drop size is not significant, indicating that generation of the secondary droplet is a random phenomenon in contrast with the impacting droplets, see Fig.4b.

For capturing all the generated secondary droplets, the measurement volume must be placed above all the splashing droplets in spray. In other words, the measurement volume must be placed above the maximum height of all possible crowns generated by splashing droplets. In Fig.6 the maximum non-dimensional crown height is presented as a function of Weber number before the impact for spray impact conditions and also for single drop impacts. Results presented in this figure indicate that the non-dimensional crown height increases linearly with Weber number before the impact. A linear correlation for non-dimensional maximum crown height in the case of spray impact condition can be given as

$$H_c^* = 3.9 \times 10^{-3} We_{nb} - 3.54 \times 10^{-2} \quad (1)$$

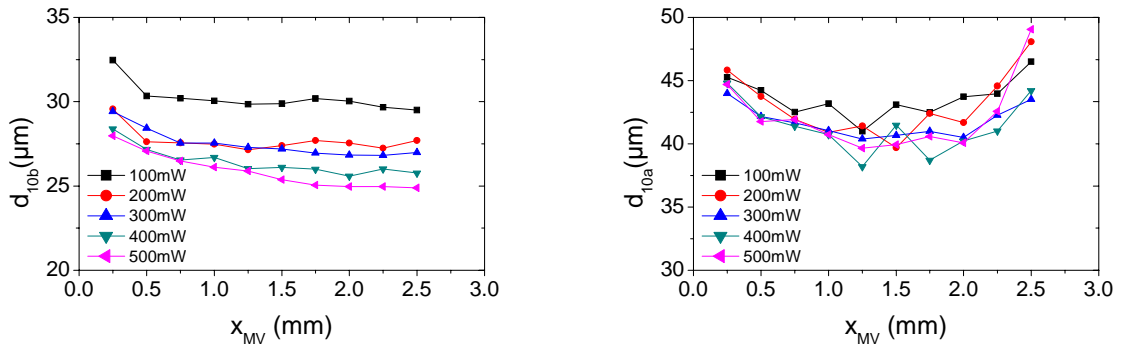


Fig. 4: Average droplet size: a) before impact, and b) after impact, as a function of measurement volume height above the rigid wall. The different lines represent different laser power.

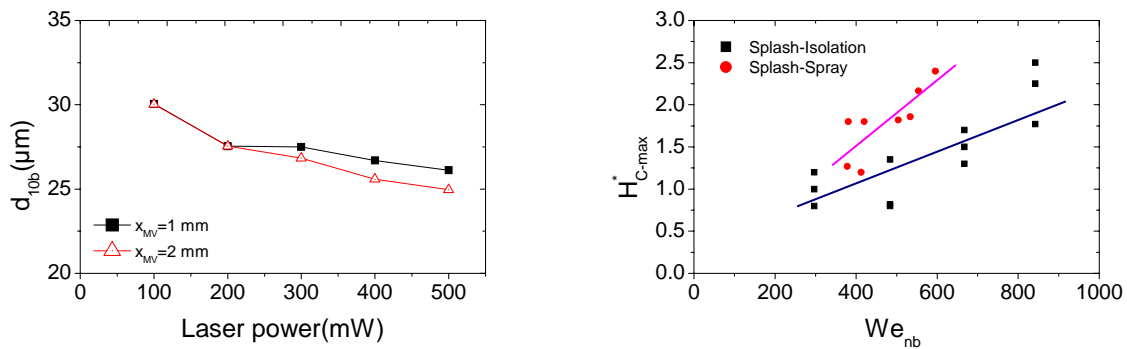


Fig. 5: Average droplet size before the impact as a function of input laser power.

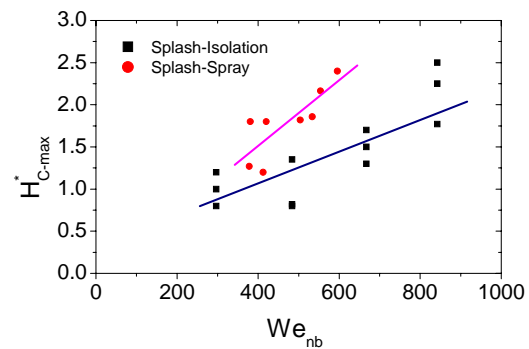


Fig. 6: Maximum non-dimensional crown height as a function of Weber number before the impact in spray and in isolation.

The difference in measuring the maximum crown height between spray impact conditions and isolation, i.e. single drop impact onto a stationary liquid film, indicates clearly that the splash created by a drop in a spray differs significantly from that of an isolated single drop impact or from the impact of a train of drops on a stationary liquid film, examined by Cossali et al. (1997) and Yarin and Weiss (1995). The source of such differences can be: tangential component of kinetic energy before the impact that exists under spray impact conditions, velocity field in the accumulated wall film, velocity fluctuations in wall film, and fluid exerted into the crown body by neighbour impacting droplets. These differences can also be easily seen in Figs.7a and b morphologically, indicating that splash of a droplet in spray impact is much more irregular and non-

symmetric in comparison to the symmetric propagation of a crown in the case of an isolated single droplet impact onto an undisturbed liquid layer.

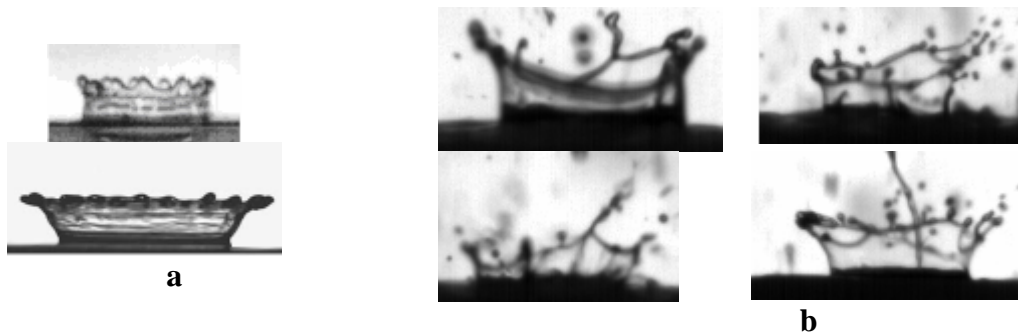


Fig.7: Morphological comparison between splashes created by a) an isolated single drop, and b) by a drop in a spray.

The total secondary-to-incident mass and number ratios show even stronger dependencies on measurement volume height above the target; hence this information is an important specification when employing such data as input data or verification data for numerical simulations. Furthermore, these dependencies can also depend on the wall film boundary conditions, i.e. on the liquid film thickness, Kalantari and Tropea (2006).

Two exemplary results are illustrated in Fig.8a and b, indicating the dependence of the total secondary-to-incident mass and number ratios on measurement volume height above the rigid wall. These results clearly indicate that total secondary-to-incident mass and number ratios decrease strongly with measurement volume height above the wall, but the influence of the laser power is not significant in most cases for both total secondary-to-incident mass and number ratios.

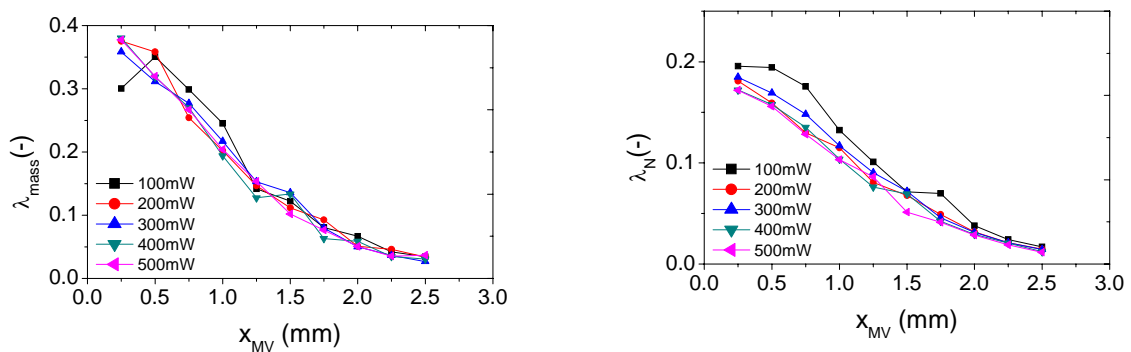


Fig. 8: Total secondary-to-incident a) mass and b) number ratios in spray impact onto a rigid wall. The different lines represent different laser power.

A second consideration is illustrated in Fig. 9 in which the positioning of a phase Doppler detection volume above an impact surface is pictured. Although highly simplified in the sense that all droplets are shown with the same velocity direction, this figure illustrates that the detected secondary droplets do not necessarily originate from the same spatial location as the detected impinging droplets. This can be of importance when high spatial gradients of the impinging spray or of the

liquid film on the wall exist, which is not unusual if the target surface is not flat. Furthermore, the drop trajectory must be accounted for when estimating the detection area size for the flux measurements, as discussed in previous publications by Roisman and Tropea (2001), and Albrecht et al. (2003).

Spatial location of the detected impinging (z_b) and secondary (z_a) spray can be expressed in the form, see also Fig.9.

$$z_b = z_0 + |x_{MV} \cdot \tan \theta_b| \quad ; \text{ for before impact} \quad (2)$$

$$z_a = z_0 - |x_{MV} \cdot \tan \theta_a| \quad ; \text{ for after impact} \quad (3)$$

where x_{MV} is measurement volume height above the target and θ_b and θ_a are average trajectory angle of impinging and secondary droplets, respectively.

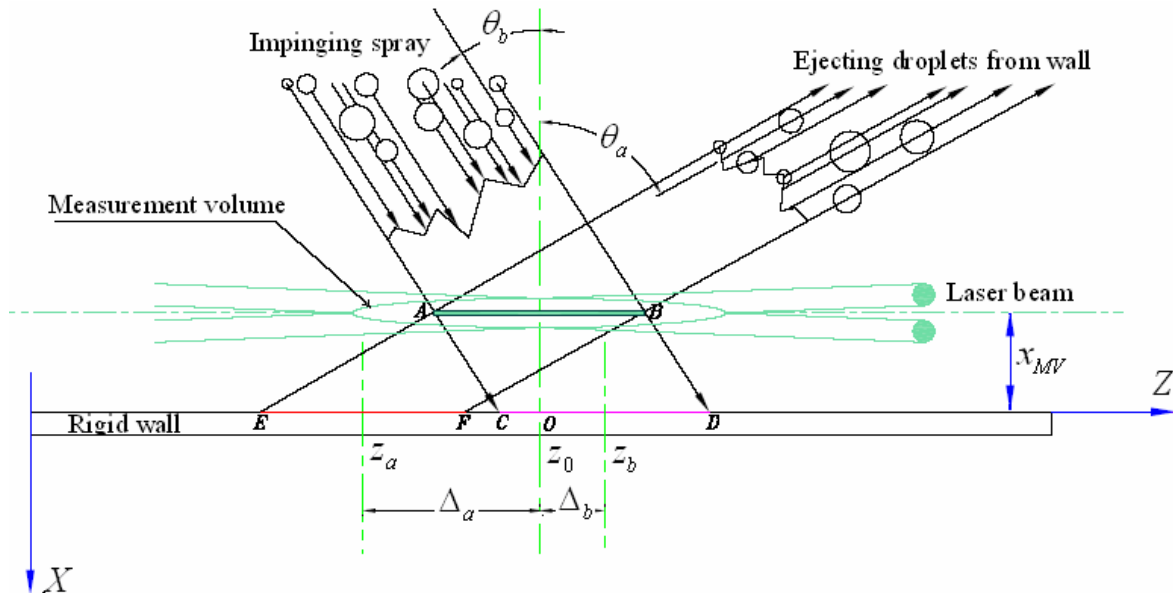


Fig. 9: Sketch for impinging and ejecting droplets passing through the detection volume.

Influence of such corrections discussed above (Eqns 2 and 3) is presented in Fig. 10a for the normal velocity component before the impact and in Fig. 10b for the normal velocity component after the impact. In these exemplary results, the measurement volume was placed 1 mm above a 15 mm rigid and flat target. As shown in this figure, the consideration is more significant for the secondary spray in comparison to the impacting spray, due to larger trajectory angles of the secondary droplets.

The average film thickness in this study was in the range $20 \mu m < \bar{h}^* < 80 \mu m$, despite the fact the Weber number before the impact varied in the range $20 < We_{nb} < 150$.

4. Conclusion

An experimental study of spray impact onto a horizontal flat and rigid surface is performed to specify the measurement volume height above the surface at which the phase Doppler data is valid. Based on the conducted experiments in this study, the suitable measurement volume height above the rigid wall can be suggested in the range between 1 mm and 1.5mm for an inertial impact condition, independent of the film thickness and target size if thin liquid film condition exists. In this region, the average after impact velocity and drop size doesn't change significantly with measurement volume height and input laser power. However, total secondary-to-incident mass and number ratios decrease significantly with measurement volume height in this region, but the influence of the laser power is not significant.

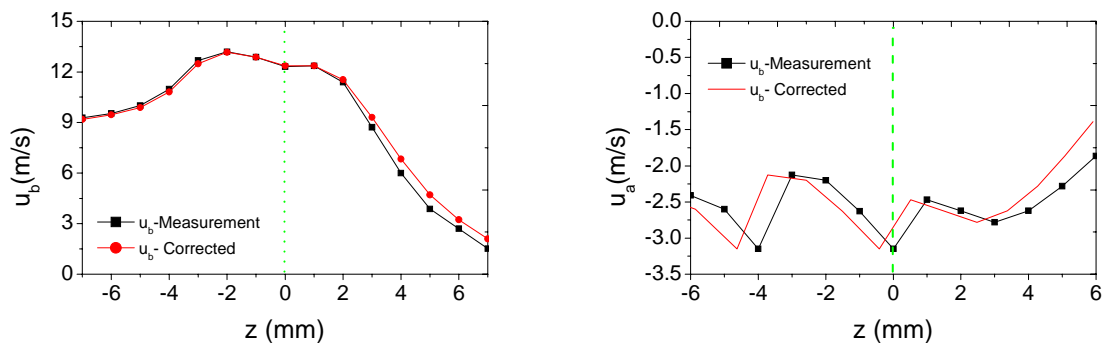


Fig. 10: Influence of correction for spatial position of the a) impinging droplet and b) secondary droplet.

A measurement volume height less than 1 mm is not recommended based on the results obtained in this study, since the characteristics of the secondary spray, e.g. average drop size and velocity, change significantly in this region. The laser power has its strongest influence on the average drop size before the impact.

5. Acknowledgments

D. Kalantari would like to thank the Ministry of Science and Technology of Iran and University of Mazandaran for financial support of his stay in Germany under scholarship No. 780274.

References

1. Albrecht, H.-E., Damaschke, N., Borys, M., Tropea, C (2003) Laser Doppler and Phase Doppler Measurement Techniques. Springer-Verlag, Heidelberg.
2. Bai, C., H. Rusche, H., Gosman, A.D., 2002. Modeling of gasoline spray impingement, *Atom. Sprays* **12**: 1-27.
3. Coghe, A., Brunello, G., Cossali, G.E., Marengo, M., 1999. Single drop splash on thin film: Measurements of crown characteristics, ILASS-Europe 99, Toulouse, July. 5-7th.
4. Cossali, G.E., Brunello, G., Coghe, A., Marengo, M., 1999. Impact of a single drop on a liquid film: experimental analysis and comparison with empirical models. Italian Congress of Thermofluid Dynamics UIT, Ferrara, 30 June-2 July.
5. Cossali, G.E., Coghe, A., Marengo, M., 1997. The impact of a single drop on a wetted surface.

Exp. Fluids **22**: 463-472.

6. Kalantari, D., Tropea, C., 2005. Experimental study of spray impact onto rigid walls, 20th ILASS-Europe, Orleans, Sept. 5-7th.
7. Kalantari, D., Tropea, C., 2006. Spray impact onto flat and rigid walls: Empirical characterization and modelling. I. J. Multiphase Flow, submitted.
8. Mundo C , Tropea C, Sommerfeld M.,1997. Numerical and experimental investigation of spray characteristics in the vicinity of a rigid wall. Elsevier 228-237.
9. Mundo, C., Sommerfeld, M., Tropea, C., 1998. On the modeling of liquid sprays impinging on surfaces, Atom. Sprays **8**:625-652.
10. Roisman I V, Tropea C. (2001) Flux measurements in sprays using phase Doppler techniques. *Atomization and Sprays*, **11**:673-705.
11. Roisman, I.V., Horvat, K., Tropea, C., Spray impact: rim transverse instability initiating fingering and splash, and description of a secondary spray, Phys. of Fluids, accepted for publication.
12. Roisman, I.V., Prunet-Foch, B., Tropea, C., Vignes-Adler, M., 2002. Multiple drop impact onto a dry solid substrate, J. Colloid Interface Sci. **256**: 396-410.
13. Roisman, I.V., Tropea, C., 2005. Fluctuating flow and jetting in a liquid layer created by an impacting spray. I. J. Multiphase Flow **31**:179-200.
14. Schmehl, R., Roskamp, H., Willman, M., Wittig, S., 1999. CFD Analysis of spray propagation and evaporation including wall film formation and spray/film. I. J. Heat and Fluid Flow **20**: 520-529.
15. Sikalo, S., Tropea, C., Ganic, E.N., 2005. Impact of droplets onto inclined surfaces. J. Colloid and Interface Science **286**: 661-669.
16. Sivakumar, S., Tropea, C., 2002. Splashing impact of a spray onto a liquid film, Phys. Fluids Lett.**14**: L85-88.
17. Sommerfeld, M. and Qiu, H. H. (1995) Particle concentration measurements by phase Doppler anemometry in complex dispersed two-phase flows. *Exp in Fluids*. **18**:187-198.
18. Stanton, D.V., Rutland, C.J., 1998. Multi-dimensional modeling of thin liquid films and spray-wall interactions resulting from impinging sprays. Int. J. Heat Mass. Trans **41**: 3037-3054.
19. Stanton, D.W., Rutland, C., 1996. Modeling fuel film formation and wall interaction in Diesel Engines. SAE paper 960628.
20. Wang, A.-B., Chen, C.-C., Hwang, W.-C, 2002. On some new aspects of splashing impact of drop-liquid surface interactions, in: Drop-surface interactions, edited by Rein, M., Springer Alert Pub.-Co.
21. Wang, M., Watkins, A.P., 1993. Numerical modelling of Diesel spray impaction phenomena. Int. J. Heat Fluid Flow **14**: 301-311.
22. Widmann, J.F., Presser, C., Leigh, S.D. (2001). Improving phase Doppler volume flux measurements in low data rate applications. *Meas. Sci. and Tech.*, **12**: 1180-1190.
23. Xu T-H, Tropea C. (1994) Improving the performance of two-component phase Doppler anemometers. *Meas. Sci. and Tech.*, **5**:969-975.
24. Yarin, A.L., Weiss, D.A., 1995. Impact of drops on solid surfaces: self-similar capillary waves, and splashing as a new type of kinematics discontinuity. J. Fluid Mech. **238**: 141-173.